CONF 930408--12

SAND92-2672C

NUMERICAL METHODS FOR FLUID FLOW IN UNSATURATED HETEROGENEOUS TUFF

Thomas H. Robey
Spectra Research Institute
1613 University Blvd., NE
Albuquerque, NM 87102
(505) 844-4441

SAND--92-2672C

DE93 006783

ABSTRACT

A numerical approach for modeling unsaturated flow is developed for heterogeneous simulations of fractured tuff generated using a geostatistical method. Cross correlations of hydrologic properties and upscaling of moisture retention curves is discussed. The approach is demonstrated for a study of infiltration at Yucca Mountain.

INTRODUCTION

Modeling flow processes at Yucca Mountain requires decisions about what physical parameters are important to include in the flow simulations. The current study seeks both to incorporate into the flow simulations the important physical processes and to tie the model more closely to actual processes ongoing at Yucca Mountain by more extensive use of field data than previous models. It also seeks to develop and demonstrate methods useful in performance assessment.

Unsaturated porous media flow in fractured tuff has a high degree of nonlinearity, which greatly increases the possibility of flow channeling. An important factor in unsaturated flow is heterogeneity, which numerical flow simulators should try to emulate. A numerical simulator based on the mixed finite element approach has been developed that attempts to preserve the basic characteristics of unsaturated flow in fractured tuff.

One of the major parameters in the performance assessments of Yucca Mountain is the infiltration rate. Yet infiltration is a difficult quantity to measure in the field. In this study, in-situ saturations are used to determine the boundary conditions, and then the numerical flow simulator calculates the corresponding infiltration rate consistent with the model.

PROBLEM DOMAIN

The domain for the flow simulation is a two-dimensional cross-section located just to the southeast of the proposed repository. The cross-section is bounded by the drill holes USW UZN-54 and USW UZN-55, which are roughly 60 meters apart. The bottom of the mesh is in the Topopah caprock while the top is the surface of the Tiva Canyon welded unit as shown in Figure 1. N-54 lies in a wash and N-55 lies to the north on the sideslope of the wash. This location suggests an infiltration higher than would be found for the proposed repository overall.

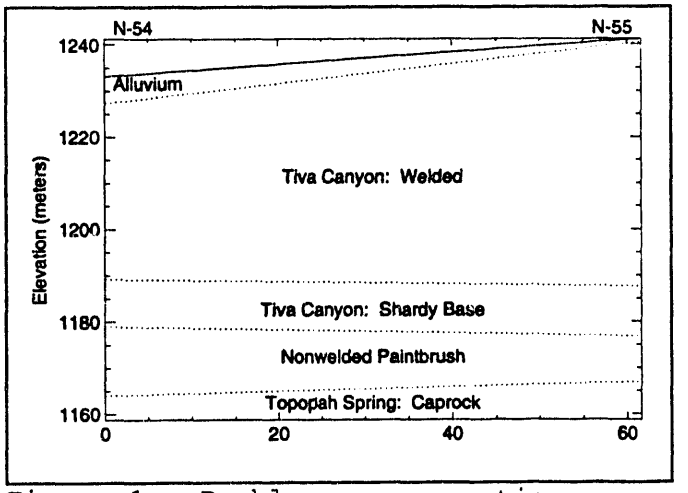

Figure 1: Problem cross-section.

It is not easy to generate heterogeneous cross-sections for the numerical flow simulator.

Heterogeneity means that field data alone will be inadequate. Also, it is desirable to maintain the spatial structure of the heterogeneity observed at Yucca Mountain. Thus, a geostatistical method of sequential Gaussian simulation conditioned to the drill hole data is used to create multiple realizations of the cross-section. The geostatistical simulation is carried out on a fine grid and then the results are upscaled to a grid suitable for the flow simulation. The grid for the flow simulation is adapted to the geostatistical simulation to minimize heterogeneity within the elements and facilitate upscaling.[1]

NUMERICAL FLOW SIMULATOR

Unsaturated flow through fractured tuff involves conductivities that change by five to eight orders of magnitude. A result of the high nonlinearity is that restriction of the path or channel cross-section can cause a higher saturation in the channel and thus, higher conductivities that can produce higher flows despite the restriction in the path.[2] Heterogeneity plays an important role in locating and exacerbating channeling.

Porous-media flow codes typically are based on finite difference or finite element methods. Such grid-based numerical methods make smoothness assumptions for certain variables. For finite differences, the use of Taylor series in its derivation assumes smoothness. In finite elements, continuity of variables is required between elements in order to assemble the global matrix from the element matrices. Most codes assume continuity for pressure which has the effect of limiting the change in pressure from element to element. Since saturation is taken to be a function of pressure, variation in saturation is also limited which inhibits channeling in the numerical simulations. To compensate, most models place many nodes or elements near material interfaces. Such techniques become much more difficult when heterogeneity is introduced and every element has different material properties. Furthermore, the nonlinearity in conductivity can cause two elements to have widely different conductivities even when their hydrologic properties are very similar.

The dual mixed finite element method enforces continuity of normal fluxes between elements but not continuity of tangential fluxes. The result is conservation of mass everywhere, including locally on element boundaries. Conservation of mass is not achieved on element boundaries when only continuity of pressure is enforced. The finite element method uses the weak or variational formulation of the differential equation, which allows the pressures to be discontinuous across element boundaries. Thus the flux-based approach does not require elements to be concentrated at material interfaces, and theoretically only a width of one element is required to resolve a channel. The resulting linearized problem is well-posed in a certain sense as long as the conductivities are bounded above and below.[3] Finite difference methods can also be derived with similar properties by avoiding differencing across cell boundaries.[4]

The dual mixed finite element method produces higher accuracy in fluxes, which is important for determining residence or travel times. Furthermore, the streamlines are more accurate; when only continuity of normal fluxes is enforced, particle paths are less likely to enter an element of low conductivity instead of going around it.[5]

Mixed finite element methods have been used with a great deal of success in porous-media flow applications such as oil reservoir modeling.[6] They are particularly successful in modeling interfaces between different fluids such as for modeling enhanced oil recovery using injection and modeling the use of bioremediation by injection of nutrients such as oxygen into hazardous waste sites.

A nonlinear two-dimensional steady state dual mixed finite element code DUAL has been assembled using an earlier linear code[3] and employing a nonlinear solver similar to that for the one-dimensional TOSPAC code[7] with additional safeguards for stability. An optional Picard solver is included to produce the intial guesses for the Newton solver. Iterative solvers do not resolve the fluxes in regions of low conductivity because of poor conditioning of the matrix; thus the use of an efficient direct method for the Picard solver is included. The

direct method involves a QR decomposition and will handle poorly conditioned or singular problems.[3]

MOISTURE RETENTION CURVE

The moisture retention curve expresses the saturation state as a function of the suction pressure. Historically, the functional relationships for unsaturated porous media have been mostly developed for soils; thus their use for fractured tuff introduces difficulties. The primary difficulty is that the curve tends to be very steep. Lab measurements often do not adequately cover the range of saturations. Fitting functions to these measurements is poorly posed because of the inadequate data.

The derivative of the moisture rentention curve expresses a functional relationship between volume-averaged pore size and suction pressure. Thus, from the moisture rentention curve, the pore size distribution can be inferred. For distributions with few data points, the mean and standard deviation are the only well-determined quantities. Parameters that determine the tails of the distribution require large numbers of data points before they can be reliably determined. The van Genuchten air entry parameter[8] depends on the largest pore size of the distribution and thus is poorly determined. This effect can be seen when fitting the van Genuchten function to moisture retention data for fractured tuff. Likewise, the residual saturation is poorly determined and can result in values as high as the lowest saturation measured (sometimes as high as 90%).

The gamma distribution is based on a mean and standard deviation. At zero the gamma function takes on the value of zero. The gamma distribution is given by

$$f(x) = \frac{\lambda(\lambda x)^{a-1} e^{-\lambda x}}{\Gamma(a)}, \quad x \geq 0,$$

where a and λ are parameters and

$$\Gamma(a) = \int_0^{\infty} e^{-u} u^{a-1}\, du.$$

At a given suction pressure at which a certain size pore desaturates, all pores of greater size are desaturated already. Thus the cumulative function is required. The incomplete gamma function

$$F(r) = \int_0^{r} f(x)\, dx = \frac{\int_0^{\lambda r} e^{-u} u^{a-1}\, du}{\Gamma(a)},$$

is the resulting moisture retention curve in terms of pore radius, r. The suction pressure is inversely proportional to the pore radius,[9] $\psi = c/r$, where

$$c = \frac{2\gamma\cos\theta}{\rho g} = 1.4185 \times 10^{-5}\ m^2,$$

and $\gamma = 0.072$ N/m is the surface tension, $\theta = 15^{\circ}$ is the contact angle, $\rho = 1000$ kg/m^3 is the density of water, and $g = 9.806$ N/kg is the gravitational constant. Substituting results in

$$F(c/\psi) = \frac{\int_0^{\lambda c/\psi} e^{-u} u^{a-1}\, du}{\Gamma(a)},$$

gives the saturation function in terms of ψ.

The mean of the gamma distribution is given by

$$\bar{r} = \frac{a}{\lambda}.$$

The standard deviation of the pore size distribution is a measure of the slope at which desaturation occurs and is given by

$$\sigma = \frac{a^{1/2}}{\lambda}.$$

Since the gamma parameters are related to the mean and standard deviation, a good fit does not require many data points. Also, since ease of computation is important, the incomplete gamma function has reasonably quick methods for its evaluation.[10]

The moisture retention curve is based on data collected from small samples. The flow simulation is based on much larger elements. In a heterogeneous environment, it is unlikely that the pore size distribution is the same for both scales. Since there are no large-scale measurements of moisture retention curves, a statistical approach is used to arrive at an appropriate curve.

Expressing the moisture retention curve in terms of the mean and standard deviation of the pore size distribution also allows the moisture retention curve to be quickly upscaled from the fine geostatistical grid to the grid used for the flow simulation. The average pore size for the larger grid is the average of the average pore sizes on the finer scale. The standard deviation of the pore size distribution for the element is given by

$$\sigma_e = \left[\frac{1}{n} \sum_{i=1}^{n} \sigma_i + (\bar{r}_e - \bar{r}_i)^2 \right]^{1/2}.$$

An implicit assumption made by the upscaling process is that the element pore size distribution can be represented by a gamma function: e.g., the distribution is not bimodal.

A moisture retention curve is shown in Figure 2 for an element with high porosity. The upscaling works well for the high porosity elements that are the most important for the simulations but appear to over predict the standard deviation of the pore size distribution for elements with low porosity. Work is ongoing to improve the numerical upscaling although ultimately field data will be required for verification.

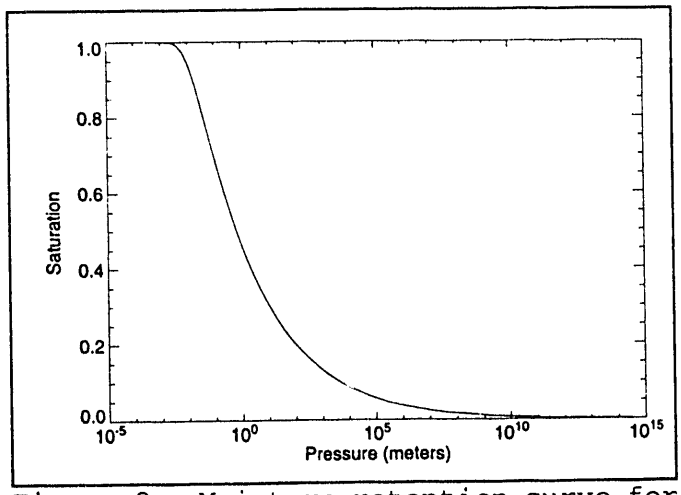

Figure 2: Moisture retention curve for element with high porosity.

CROSS CORRELATIONS

The hydrologic properties are interrelated. Thus, to more closely match the actual process, the variables should be correlated with each other. Both porosity and saturated conductivity are covered in the another paper on geostatistics.[1] The appropriate functional relationship between the other variables is not as well understood. Data from Yucca Mountain[11,12,13,14] and an analog site[15] are used as a basis for the correlations. It is important to include data from several studies since each study tends to have their own calibration ranges and biases. Samples thought to contain zeolites are omitted since the problem domain does not include the zeolitic unit. The data for porosity, ϕ, saturated hydraulic conductivity, k_s, and average pore size, $\bar{r}$, are plotted in Figure 3. The average pore size for the fine grid is calculated from

$$\ln k_s = 9.26 + \ln(\phi \bar{r}^2) + R_1(x)$$

where $R_1(x)$ is a random number sampled from

$$p_1(x) = \frac{1}{\sqrt{2\pi}} e^{-\frac{1}{2}\left(\frac{x}{1.78}\right)^2}.$$

In Figure 4, the average and standard deviation of the pore size distribution are plotted. They appear to be correlated very strongly, i.e., the

fitted gamma functions appear to reduce to a one parameter family at this scale. This could either be an artifact of the fitting process or there may be an underlying structural reason. A physical reason for the strong correlation may be that each size pore has a surface roughness thus providing smaller and smaller pores in a structured way. The standard deviation is calculated using

$$\ln \sigma_i = 0.597 + 1.08 \ln \bar{r}_i + R_2(x),$$

where $R_2(x)$ is a random number sampled from

$$p_2(x) = \frac{1}{\sqrt{2\pi}} e^{-\frac{1}{2}\left(\frac{x}{0.482}\right)^2}.$$

The average and standard deviation of the pore size distribution have been calculated at the fine scale of the geostatistical grid and now must be upscaled to the flow grid. Since the error is in terms of exponentials, the upscaling uses the natural log of the average and standard deviation (geometric average). In upscaling σ it was found that uncertainty in calculating $\bar{r}$ dominated the result so all the random noise is omitted.

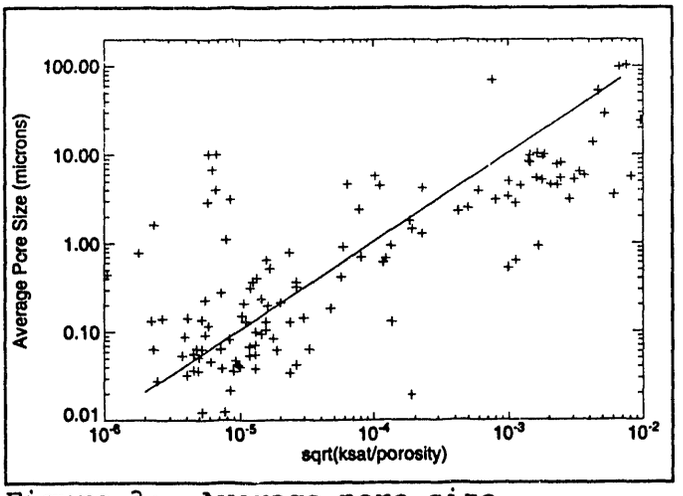

Figure 3: Average pore size.

The unsaturated conductivity requires computation of $k_r = k/k_s$. The most common methods are due to Mualem[16] and Brooks and Corey.[17] There are very few data for unsaturated conductivity, so the Brooks and Corey method is used since the integration of the incomplete gamma function required for Mualem's method would be slow. Klavetter and Peters[9] determined the Brooks-Corey constant, ε, for five samples of tuff from Yucca Mountain using the van Genuchten function. From this data

$$\varepsilon = 6.66 - 5.08\phi + R_3(X),$$

where $R_3(x)$ is a random number sampled from

$$p_3(x) = \frac{1}{\sqrt{2\pi}} e^{-\frac{1}{2}\left(\frac{x}{0.745}\right)^2}.$$

The fracture parameters have more uncertainty because of the difficulty in observing fractures in-situ. The van Genchten parameters of α = 1.28, β = 4.23 and s_r = 0.04 have been used in several previous studies. Taking several data points and fitting a gamma function results in a = 4.81 and λ = 0.381. Since fracture flow was not observed in the results, the other fracture properties are omitted from discussion.

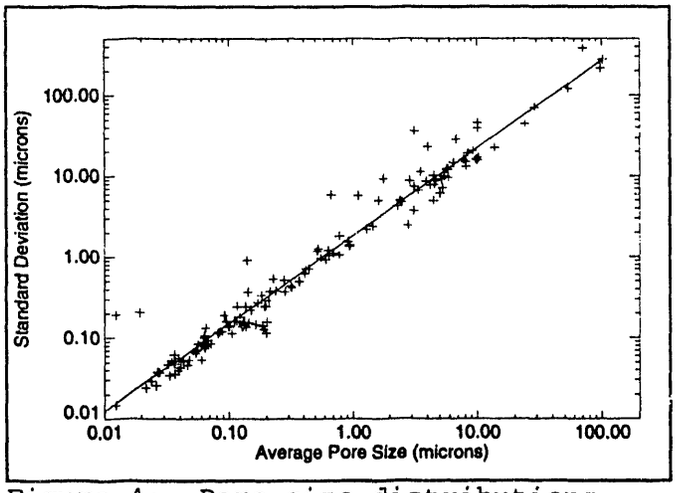

Figure 4: Pore size distributions.

BOUNDARY CONDITIONS

Typically, most flow simulations vary a uniform infiltration rate until the simulation state variable, saturation, matches in some sense the in-situ saturations. However, it is very unlikely that the infiltration is uniform. One study[18] divides the surface into three infiltration zones: alluvium, sideslope and ridgetops. Yet even in these zones it is very unlikely that infiltration is close to uniform. Furthermore, it is very difficult to

measure infiltration in the field, so performance assessment is subject to continuing questions about the proper value for infiltration.

The best indicators of the current state of the hydrologic system at Yucca Mountain are the in-situ saturations: thus they are used to determine the boundary conditions for these flow simulations. Since pressures are discontinuous across elements for the dual mixed finite element method, the pressure boundary conditions determined by the in-situ saturations are easily incorporated. The flux field and infiltration are produced as output by the numerical flow simulator.

On the left and right sides of the problem domain the saturations are converted to pressures. Since moisture retention data are not provided for core samples where in-situ saturation were obtained, then a moisture retention curve based on the scale of the fine geostatistical grid is used. The standard deviation of the appropriate pore size distribution is the average standard deviation for all the data points in the element. The pressure on the boundary for each element is taken to be the median pressure of all converted pressures lying on the side of the element. Thus the pressure boundary conditions are determined by field data but are not very sensitive to outliers.

Part of the top of the problem domain lies under alluvium while the rest is sideslope. The pressure derived from the saturation at the top of N-55 (69%) is used as the boundary condition for the 15-meter-wide alluvium. For the sideslope, the pressure derived from the saturation at the top of N-54 (30%) is used. Since saturation and moisture retention curves at the surface can be measured in the field, these values can be verified by gathering more data.

The pressure at the bottom of the mesh is assumed to vary linearly. The pressures for either end are taken to be the same as for the side of that element. This boundary condition assumes that the bottom of the mesh lies in the Topopah caprock.

RESULTS

Seven geostatistical simulations are generated using different seeds. For the two seeds 1713 and 1723 the Topopah caprock is not intact along the bottom of the mesh. The pressure, unsaturated conductivity, and matrix saturation for seed 1711 produced by the numerical flow simulator are shown in Figures 5, 6 and 7, respectively. The results of the flow simulation follow the general trends in the data from the drill holes except for details in the capillary barrier above the nonwelded Paintbrush interval. At the bottom of the Tiva Canyon welded unit is the shardy base, which gradationally becomes nonwelded. The field data shows the top of the shardy base is nearly saturated. The simulation shows a capillary barrier but not the increased saturation just above it. The problem could be due to lack of resolution of the numerical flow simulation or averaging inherent in the geostatistical simulator. The flux field for seed 1711 is shown in Figure 8. Infiltration occurs in the alluvium and exfiltration along the sideslope. The flow in the nonwelded Paintbrush interval is towards the south. The two large vectors are due to inaccuracies in the boundary conditions in an area of high variability.

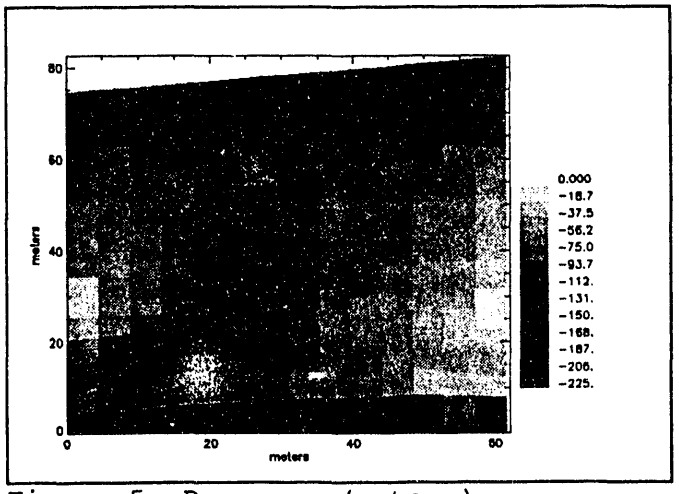

Figure 5: Pressure (meters).

Although the flow fields in the simulations are quite complex, the infiltration at the bottom of the mesh is reasonably uniform. For the five simulations with an intact Topopah caprock the infiltration ranges between 1.3 mm/yr and 2.8 mm/yr. This infiltration rate is considered conservatively high since the problem domain is in a wash and the horizon at which the infiltration rate is calculated is just one element width below the nonwelded Paintbrush unit.

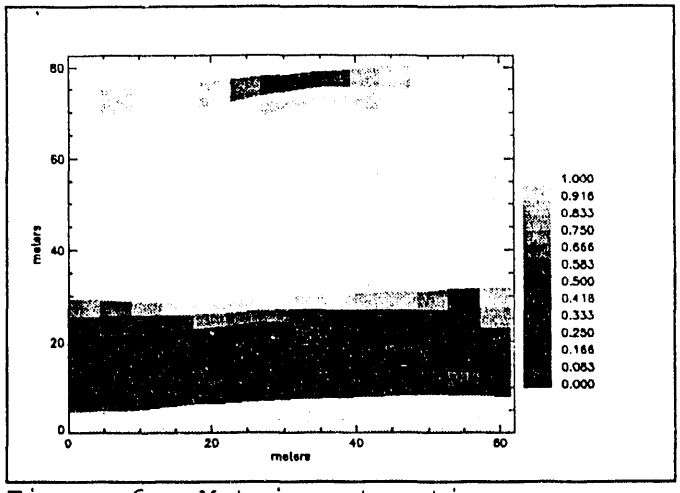

Figure 6: Matrix saturation.

Horizontal flow is important in this simulation as the average ratio of horizontal to vertical flow over the entire mesh is greater than 4.5 for all seven simulations.

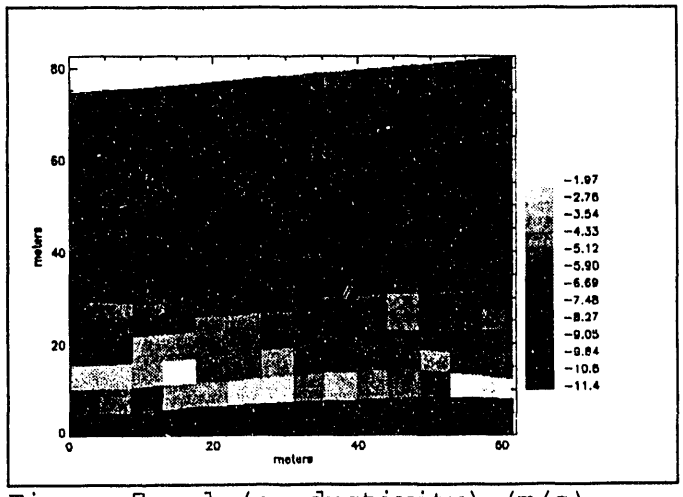

Figure 7: ln(conductivity) (m/s).

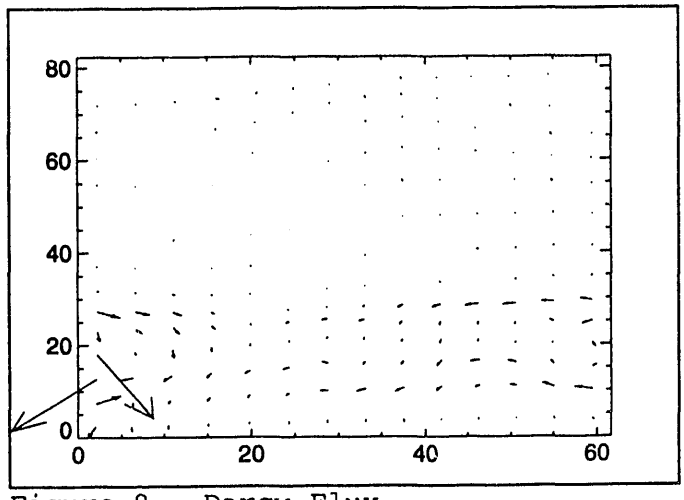
Figure 8: Darcy Flux.

For seed 1711, a flow grid of 7 by 7 is used for evaluating the effects of grid resolution on the silulated infiltration. The simulations are generally comparable although a few elements are affected by the lack of resolution in the boundary conditions. The infiltration is -8.0 mm/yr instead of -1.9 mm/yr for the 14-by-14-element grid. The increased resolution results in less infiltration which is the intuitive result for flux-based methods without channeling.

The interface between the nonwelded Paintbrush interval and the Topopah caprock is quite sharp in the five simulations where the caprock is intact. The capabilities of the dual mixed finite element method are demonstrated along this interface since pressure and saturation abruptly change at the interface without the use of small elements. There also is a very distinct difference in the flux fields on either side of the interface with primarily horizontal flow above and primarily vertical flow in the caprock. Channeling within the caprock in the simulations with an intact caprock is only found for seed 1717. The ability of flux based methods to model channeling in unsaturated porous media flow is shown in Figure 9. Although infiltration is not greatly affected by the channeling, a larger impact could be expected on travel times.

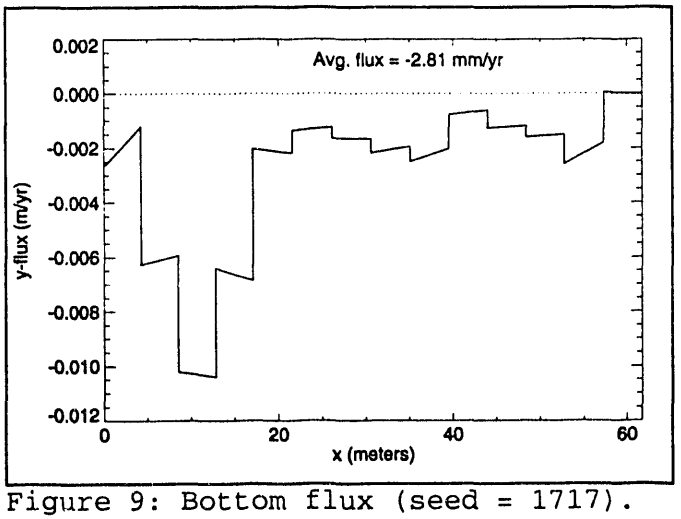

Figure 9: Bottom flux (seed = 1717).

When the Topopah caprock is not intact in the geostatistical simulation, the assumptions for the bottom boundary are violated, and it is not possible to determine infiltration in the caprock. However, the results for these two simulations are interesting. Figure 10 shows the flux at the bottom of the mesh for seed 1723. In the center of the break the high saturated conductivity causes the

saturation to decrease and low fluxes result. The high fluxes occur at the edges of the high porosity region where the saturated conductivity is not so high that the available water in the nonwelded Paintbrush can support the flows.

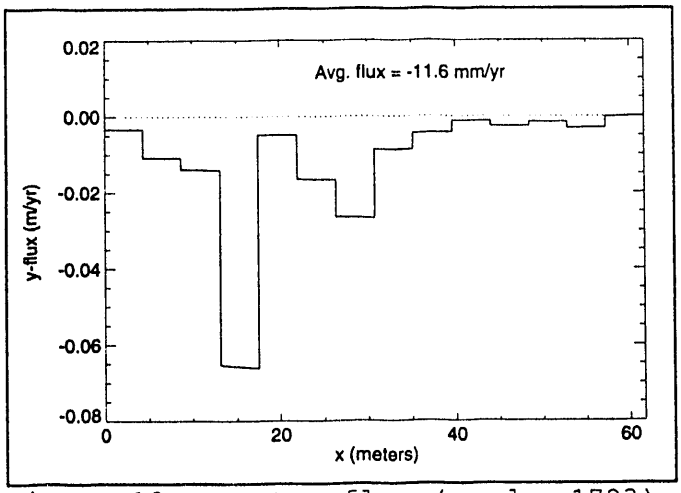

Figure 10: Bottom flux (seed = 1723).

CONCLUSIONS

Numerical methods appropriate for unsaturated flow in heterogeneous tuff have been developed and demonstrated. The flux-based flow simulator allows for channeling, which can be seen in a few places in the results. It has also been shown that numerical flow simulators can handle the complex heterogeneous input generated by geostatistical methods.

A two-dimensional numerical flow simulation is applied to heterogeneous geostatistical simulations of a cross-section between two drill holes. The cross-section reaches to the Topopah caprock where the infiltration is simulated. The simulation shows that both infiltration and exfiltration occur at the surface of the tuff, but in the Topopah caprock the flux is much more uniform. These results provide a conservative estimate of appropriate infiltration values and suggest that one-dimensional analysis may be appropriate below the repository horizon.

ACKNOWLEDGEMENT

This work was performed at Sandia National Laboratories for the U. S. Department of Energy, Office of Civilian Radioactive Waste Management, Yucca Mountain Site Characterization Project, under contract DE-AC04-76DP00789.

REFERENCES

1. C. A. RAUTMAN and T. H. ROBEY, "Recent Developments in Stochastic Modeling and Upscaling of Hydrologic Properties in Tuff", *High Level Radioactive Waste Management, Proceedings of the Fourth International Conference* (1993).

2. R. C. DYKHUIZEN and R. R. EATON, "Effect of Material Heterogeneities on Flow Through Porous Media", *High Level Radioactive Waste Management, Proceedings of the Second International Conference* (1991).

3. T. H. ROBEY, *The Mixed Finite Element Method*, Ph. D. Dissertation, University of New Mexico (1990).

4. J. E. MOREL, J. E. DENDY, M. L. HALL and S. W. WHITE, "A Cell-Centered Lagrangian-Mesh Diffusion Differencing Scheme", *LA-UR-90-3582*, Los Alamos National Laboratory (1990).

5. E. F. KAASCHIETER and A. J. M. HUIJBEN, "Mixed Hybrid Finite Elements and Streamline Computation for the Potential Flow Problem", *Numerical Methods for Partial Differential Equations*, *8*, 221 (1992).

6. M. F. WHEELER and R. GONZALEZ, "Mixed Finite Element Methods for Petroleum Reservoir Engineering Problems", *Computing Methods in Applied Sciences and Engineering, IV*, ed. by R. Glowinski and J.-L. Lions, Elsevier Science Publishers B. V., 639 (1984).

7. A. L. DUDLEY, R. R. PETERS, J. H. GAUTHIER, M. L. WILSON, M. S. TIERNEY and E. A. KLAVETTER, "Total System Performance Assessment Code (TOSPAC) Volume I: Physical and Mathematical Bases", *SAND85-0002*, Sandia National Laboratories (1988).

8. R. VAN GENUCHTEN, "Calculating the Unsaturated Hydraulic Conductivity with a New Closed Form Analytical Model", *Water Resources Bulletin*, Princeton University Press (1978).

9. E. A. KLAVETTER and R. R. PETERS, "Estimation of Hydrologic Properties of an Unsaturated, Fractured Rock Mass", *SAND84-2642*, Sandia National Laboratories (1984).

10. W. H. PRESS, B. P. FLANNERY, S. A.

TEUKOLSKY and W. T. VETTERLING, *Numerical Recipes in C*, Cambridge University Press, Cambridge (1988).

11. YUCCA MOUNTAIN PROJECT, "Data Resulting from Data Acquisition", *Technical Data Information Form*, DTN GS920508312231.010 (1992).

12. R. R. PETERS, E. A. KLAVETTER, I. J. HALL, S. C. BLAIR, R. R. HELLER and G. W. GEE, "Fracture and Matrix Hydrologic Characteristics of Tuffaceous Materials from Yucca Mountain, Nye County, Nevada", *SAND84-1471* (1984).

13. L. E. FLINT and A. L. FLINT, "Preliminary Permeability and Water-Retention Data for Nonwelded and Bedded Tuff Samples, Yucca Mountain Area, Nye County, Nevada", *U. S. Geological Survey Open-File Report 90-569* (1990).

14. B. M. RUTHERFORD, I. J. HALL, R. R. PETERS, R. G. EASTERLING and E. A. KLAVETTER, "Statistical Analysis of Hydrolgical Data for Yucca Mountain", *SAND87-2380* (1992).

15. A. K. STOKER, W. D. PURTYMUN, S. G. McLIN and M. N. MAES, "Extent of Saturation in Mortendad Canyon", *Los Alamos Report LA-UR-91-1660* (1991).

16. Y. MUALEM, "A New Model for Predicting the Hydraulic Conductivity of Unsaturated Porous Materials", *Water Resources Research, 12*, 513 (1976).

17. R. H. BROOKS and A. T. COREY, "Properties of Porous Media Affecting Fluid Flow", *Journal of the Irrigation and Drainage Division, Proceedings of the American Society of Civil Engineers, IR2*, 61 (1966).

18. C. S. WITTWER, G. S. BODVARSSON, M. P. CHORNACK, A. L. FLINT, L. E. FLINT, B. D. LEWIS, R. W. SPENGLER and C. A. RAUTMAN, "Design of a Three-Dimensional Site-Scale Model for the Unsaturated Zone at Yucca Mountain, Nevada", *High Level Radioactive Waste Management, Proceedings of the Fourth International Conference* (1992).

END

DATE
FILMED
4/3/93